Proceedings of the ASME 2010 3rd Joint US-European Fluids Engineering Summer Meeting and 8th International Conference on Nanochannels, Microchannels, and Minichannels
FEDSM-ICNMM2010
August 1-5, 2010, Montreal, Canada

FEDSM-ICNMM2010-30480

SIMULATION OF FLOW-INDUCED ACOUSTIC RESONANCE OF BLUFF BODIES IN DUCT FLOW

Erick Reyes
Department of Mechanical and Manufacturing Engineering
Trinity College Dublin
Ireland
reyescae@tcd.ie

Shane Finnegan
Department of Mechanical and Manufacturing Engineering
Trinity College Dublin
Ireland
finnegsl@tcd.ie

Craig Meskell
Department of Mechanical and Manufacturing Engineering
Trinity College Dublin
Ireland
cmeskell@tcd.ie

ABSTRACT

It is well known that the periodic vortex shedding from bluff bodies in a duct can excite the transverse acoustic mode if the frequencies are comparable. There is a considerable body of experimental work investigating this phenomenon for multiple cylinders. Numerical studies are somewhat less common, partially because it is difficult to couple the acoustics and the hydrodynamic field. This paper implements a hydrodynamic analogy proposed by Tan et al. in which the acoustic field is represented by a velocity excitation of the incompressible hydrodynamics at the domain extents. Two alternatives to this boundary condition are considered: rigid body vibration and surface potential flow. In all three cases, the flow field for two tandem cylinders with a spacing ratio of 2.5D has been simulated with uRANS and an RSM turbulence model. It has been found that a rigid body vibration is not a good model of acoustic excitation. However, imposing a potential flow at the surface of the cylinders yields promising results. The success of the new boundary condition implies that the coupling between the acoustic field and the hydrodynamics is not reorganizing the wake directly, but rather simply modifying the generation of vorticity at the surface. Furthermore, it is envisaged that the new modeling approach will be easier to implement for complex geometries, such as tube arrays.

INTRODUCTION

The effect of acoustic resonance on bluff bodies is a topic of significant interest in many industrial applications such as tubes arrays in heat exchangers, where the tubes are subject to cross flow. Due to the bluff body geometry periodic vortex shedding is to be expected. The frequency of the vortex shedding can affect the system in different ways, from a simple vibration and noise case, it might be tolerant in some applications, to fatigue failure of the materials in some others if its frequency matches the natural frequency of the system.

Acoustic sources can interact with the fluid due to the nature of the acoustics, a pressure wave applied to the fluid. The flow and the geometry create a natural vortex shedding phenomenon. An acoustic excitation added to the system modifies the behaviour of the vortex shedding, and in some conditions the acoustics have the ability to modulate and in some way control the frequency of the vortex shedding, a phenomenon known as "lock-in" process. This could lead to acoustic resonance of the system with the corresponding consequences attached to it.

Vortex shedding and "lock-in" process have received much attention in the literature. For example, Mohany and Ziada [1], Hall et al. [2], Finnegan et al. [3] have completed experimental and numerical investigations of the sound interaction on cross flow cylinders. Hourigan et al. [9] used a Lagrangian vortex particle method to simulate the unsteady flow around baffles, with the acoustic particle velocity added during the convection of the vorticity particles. The method provided very good insight to the feedback mechanisms, however, the method required the infinite velocities associated with the vortex particles to be arbitrarily curtailed. Tan et al. [8] solved this problem by using a DNS solution of a low Reynolds number flow around a horizontal baffle plate in a duct. The effect of the acoustic field was imposed by superimposing a transverse sinusoidal velocity on the outer boundaries (i.e. away from the bluff body) of the mesh. A similar approach has been used successfully by Mohany and Ziada [1] for turbulent flow around tandem cylinders using uRANS solver.

The "lock-in" process and the interaction of the acoustic power is well understood phenomenon within the scientific community for a single cylinder [1]. Nevertheless for more complex structures there is research in progress to understand the behaviour of the acoustic and hydrodynamic fields within the couple flow field and the effect of the geometry on the results compared to the isolated case. Mohany and Ziada [4] and Finnegan et al. [3] have examined two tandem cylinders. experimentally.

The experimental setup of these multiple cylinder configurations is more complex than the single case and numerically it demands a higher level of computational resources because of the variables and the amount of data required. In order to overcome these factors, the purpose of this work is to develop and test an equivalent numerical model applying the forces directly on the surface of the cylinders. Where possible, the models have been validated against the experimental data available. The ultimate objective is to provide a tool for design and research on aeroacoustics interactions at relative small velocity ratios, in complex geometries, which is a scenario that is difficult to realize experimentally.

The difficulty with the numerical simulation approaches used to date is that the effect of the acoustic field on the hydrodynamics is modeled by a periodic boundary condition at the outer extent of the flow domain. This is problematic for two reasons: firstly the velocity excitation occurs at a location which may be an acoustic velocity node; and secondly, the entire flow field is excited via the viscous momentum equation. A practical problem is that the method used by Mohany and Ziada [1] requires relatively high levels acoustic particle velocity to achieve lock-in, and so the method as it exists can not form the basis of reliable estimates of resonance amplitude. In this paper two alternative boundary conditions to model the acoustics are proposed, both of which are applied at the cylinder surface not the domain limits. The performance of all three modeling approaches is assessed for a range of frequency ratios and excitation amplitudes for a single tandem cylinder configuration.

BACKGROUND THEORY

The aeroacoustic "lock-in" is a phenomenon present in hydrodynamic and acoustic interactions. It occurs when the frequency of the vortex shedding, f_v, approaches the acoustic frequency, f_a, combining both frequencies with the ability of the acoustics to somehow modulate and control the vortex shedding.

Mohany and Ziada [1] found that the "lock-in" range of the two tandem cylinders is wider than the single cylinder case. The extent of "lock-in" zone depends on the amplitude of the oscillation velocity and the ratio of the acoustic and vortex shedding frequencies.

Figures 1 and 2 show examples of the time and frequency responses, respectively in a "lock-in" regime, while Figures 3 and 4 show the equivalent traces for a "not lock-in" process. All these figures are based on the response of the lift coefficient on the downstream cylinder. Note that as the simulations are 2D, the amplitude of the lift coefficient will be significantly over estimated, as in effect an infinite correlation length is imposed.

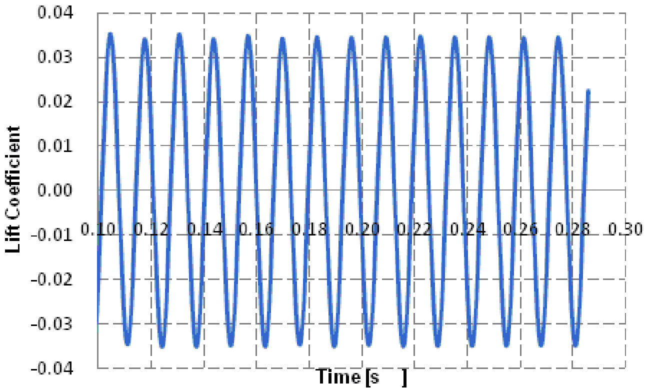

Figure 1. Typical lift coefficient time record - "lock-in" behavior. Acoustic excitation amplitude: 2%; frequency ratio (f_a/f_v)=0.875.

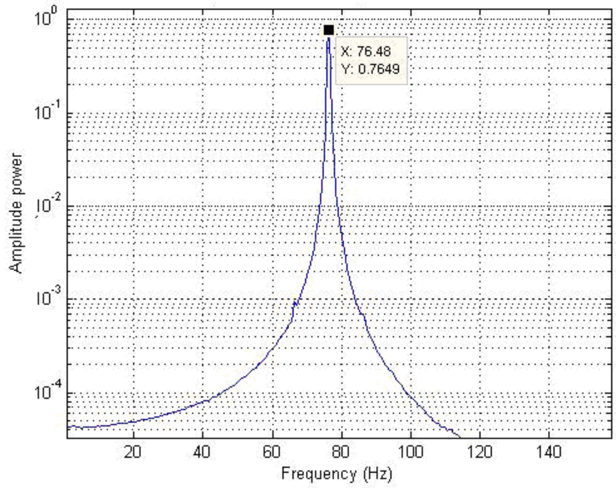

Figure 2. Typical "lock-in" lift coefficient power spectrum. Acoustic excitation amplitude: 2%; frequency ratio (f_a/f_v)=0.875.

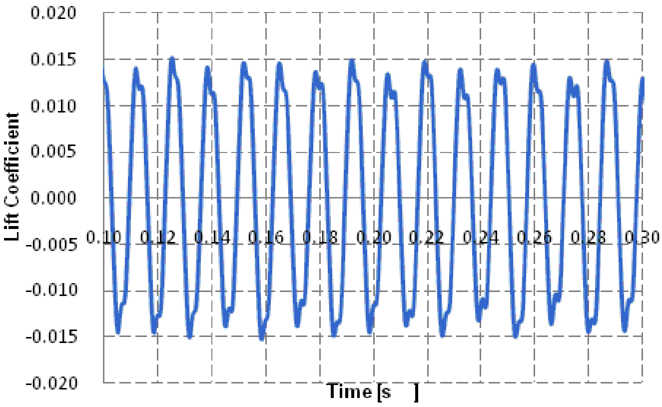

Figure 3 Typical not "lock-in" lift coefficient time record. Acoustic excitation amplitude: 2%; frequency ratio (f_a/f_v)=1.4.

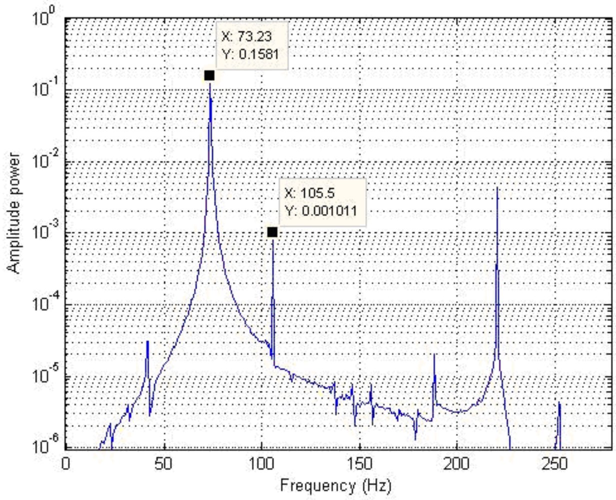

Figure 4. Typical not "lock-in" lift coefficient power spectrum. Acoustic excitation amplitude: 2%; frequency ratio (f_a/f_v)=1.4.

The aerodynamic acoustic power is calculated using Howe's theory of aerodynamic sound [10]:

$$\Pi = -\rho \int \vec{\omega}.\left(U_a \times \vec{V}\right) d\Re \qquad (1)$$

Where Π is the instantaneous acoustic power and the result of the triple product between the vorticity vector $\vec{\omega}$, the acoustic particle velocity vector U_a and the flow velocity vector $\vec{V}$, where ρ is the mean density of the flow volume $\Re$. The net acoustic energy is the result of the integral the time resolving acoustic power over the entire wave cycle.

NUMERICAL TECHNIQUE

The geometry chosen to explore the boundary conditions was representative of the wind tunnel installation of a two tandem cylinder configuration with diameter D=25.4mm at a pitch ratio of P/D=2.5, which was studied by Mohany & Ziada[1,4]. The simulation boundaries are located at ±5D in the cross flow direction, 5D upstream and 20D downstream with the upstream cylinder as reference point of view as shown schematically in Figure 5(a).

The basic modeling approach is to solve for the instantaneous acoustics velocity and the hydrodynamic components separately. In order to retain the interaction between the acoustics and hydrodynamics, the hydrodynamics are forced with an additional boundary condition. Figure 5 shows a schematic of the overall modeling approach.

The model and mesh were created using GAMBIT 2.4.6 and the simulation of the flow field was performed in FLUENT 6.3.26 using the RSM turbulent model. This is a seven equation turbulent model, it does not assume isotropic turbulence and Reynolds stress transport equation can account for the directional effects of the Reynolds stress field. It has superior performance in near wall modeling because it can predict the viscous effects on the wall approach.

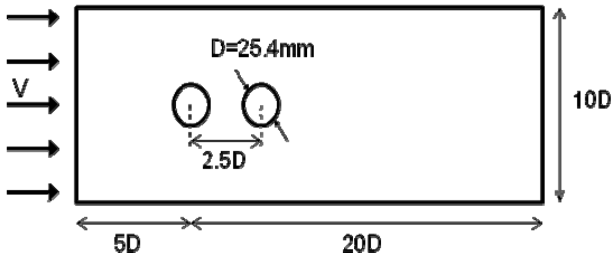

(a) Geometry of domain.

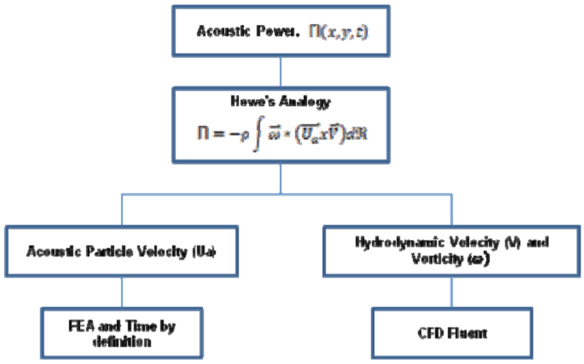

(b) Modeling approach.

Figure 5. Schematic of numerical model.

The simulations were performed in a two dimensional model at a Reynolds number of 25,000 for the hydrodynamic field. Based on the Reynolds number, the mean flow velocity at the flow inlet is 14.377 m/s, for a cylinder diameter of 25.4mm. The properties of the working medium, air, set in FLUENT are density ρ=1.225 kg/m^3 and a viscosity μ=1.7894x10^{-5} kg/m-s. The solution controls set up for the simulation were second-order momentum in discretization criteria, PISO algorithm for the pressure-velocity coupling and Low-Reynolds number wall approach for the viscous model.

In order to validate the hydrodynamics model, several simulations were conducted at different Reynolds numbers, setting one velocity inlet and one outlet in the *x*-direction without acoustic excitation. The performance of the vortex shedding obtained during this process agrees well with the experimental data described in the literature. The frequency of the vortex shedding, f_v, was determined using the record of the lift coefficient on the downstream cylinder; the result obtained is 75.4 Hz. This frequency will be a key point of reference for setting the acoustic frequency in the system.

In order to simulate the acoustic field interacting with the hydrodynamics, a secondary boundary condition is applied to the simulation in terms of velocity perturbation using a temporal sinusoidal wave corresponding to the acoustic particle velocity. The hydrodynamic field is extracted from FLUENT. The acoustic pressure mode shape is obtained from ANSYS software applying finite element model of the tunnel with the cylinders in it; the acoustic database and model used in this work in order to combine and obtain the spatial acoustic power distribution correspond to the previous work of Finnegan et al. [3]. Both databases and meshes were reorganized and combined onto a structured grid in MATLAB software. The acoustic particle velocity, U_a, was determined by solving the Euler equation:

$$\rho \frac{\partial U_a}{\partial t} = -\nabla Pa \quad (2)$$

Where ρ is the mean density of air, t is the time and ∇Pa is the gradient of the acoustic pressure. Thus, all three elements of Howe's equation (Eq. 1) are available at each time step and so the instantaneous spatial distribution of the acoustic power can be obtained.

Three different boundaries conditions were evaluated using the basic model and properties described above. For all scenarios the applied acoustics are simulated through the hydrodynamics in the system, as a secondary velocity inlet or boundary condition applying a sinusoidal velocity condition as a User Defined Function (UDF), in FLUENT. The timebase of this function is simply the physical time record in the simulation. Ultimately, the excited hydrodynamics are combined with the acoustic field in MATLAB as a post-processing operation to yield the instantaneous spatial distribution of acoustic power.

Boundary condition 1 – Cross-flow. The first boundary condition is a cross-flow model, with a constant mean flow velocity inlet in the *x*-direction based on Reynolds number. The cross-flow is a sinusoidal velocity inlet condition in the *y*-direction on the top and bottom surfaces. Figure 6 shows the configuration of this model schematically. It is similar the model that has been used by, Tan et al. [8] and Mohany and Ziada [1]. This approach excites the entire flow field directly through the viscous momentum equation.

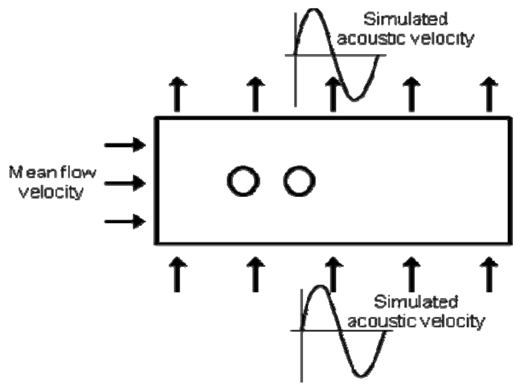

Figure 6. Diagram of cross flow boundary condition

Boundary condition 2 – Rigid body vibration. The second approach adopted assumes that the acoustic excitation is analogous to rigid body vibration. Thus, the effect of the acoustics is modeled as a sinusoidal velocity at the surface of each cylinder. At every instant, the velocity over the entire surface of the cylinders is the same, and is in general. Figure 7 presents this scheme schematically.

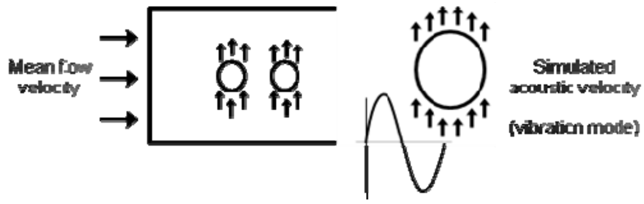

Figure 7. Diagram of vibration boundary condition of the cylinders

Exactly the same UDF as was used for the cross-flow condition to set a fluctuating velocity inlet in the *y*-direction at the mesh extents can be applied to the moving wall condition, simply by setting the *y*-component of the UDF to the instantaneous vibration velocity and the *x*-component to zero.

Boundary condition 3 – Surface acoustic flow.

The acoustic field induces an irrotational flow field throughout the domain and at the surface of the cylinder. In this boundary condition, it is assumed applying the instantaneous acoustic particle velocity at the surface will capture the important interaction with the hydrodynamics. This will obviously violate the no-slip condition. However, in the absence of viscous flow, it can be considered that the acoustic velocity is non-zero immediately outside a very thin boundary layer. The assumption implicit in this boundary condition is effectively that this boundary layer is sufficient thin as to be negligible. Figure 8 shows the schematic for this model.

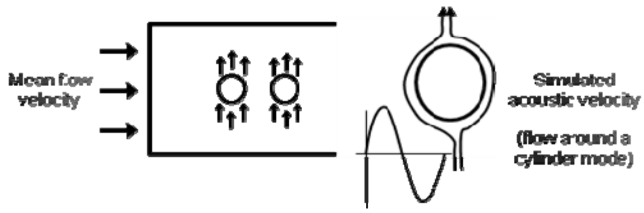

Figure 8. Diagram of simulated boundary condition for surface acoustic flow.

While it is possible to extract the acoustic particle velocity at the surface of the cylinder, and indeed it is available from the FE analysis, in order to simplify the implementation of the surface acoustic flow boundary condition, a surface flow equivalent to an isolated cylinder in potential flow is applied. Thus, the tangential surface velocity applied in this boundary condition is simply

$$U_a(t) = 2\left|U_a\right|\sin\theta \quad (3),$$

where U is the instantaneous flow velocity at every point of the boundary layer, U_0 is the mean flow velocity en direction to the cylinders and θ, is the anglar location relative to each cylinder centre. Note that θ is zero at the top of each cylinder.

This approach is reasonable because the wavelength of the acoustic field is large compared to the tube diameter and the tube spacing is such that the interaction of the acoustic flow field around each cylinder is weak. When compared with the acoustic velocity calculated numerically (from FE and extrapolating to the surface) the difference is small.

RESULTS - COMPARISON OF BOUNDARY CONDITIONS.

Instantaneous behaviour. The simulations were run for a sufficiently long time such that start up transients had decayed, and the remaining data offered spectra with a frequency resolution of 0.366Hz.

Figure 9 shows a comparison between the velocity, vorticity and spatial distribution of acoustic power for the three boundary conditions at pre-coincidence acoustic resonance, all profiles are taken at the same phase (0^o) relative to the acoustic particle velocity. Qualitatively, the “cross flow” and “surface acoustic flow” conditions are quite similar. However, the rigid body vibration condition displays significant differences: the positive vorticity shed from the upstream cylinder is impinging substantially on the downstream cylinder; the downstream wake is out of phase compared to the other the other conditions; the acoustic power map shows an intense source region immediately behind the upstream cylinder while the other two boundary conditions show a much smaller source region and a larger sink region.

Figure 10 shows the velocity, vorticity and spatial distribution of acoustic power for a half-cycle at coincidence acoustic resonance for the “surface acoustic flow” model, with the acoustic pressure as reference for the phase. The instantaneous spatial distribution of all three quantities compares well with the experimental data obtained by Finnegan et al. [3].

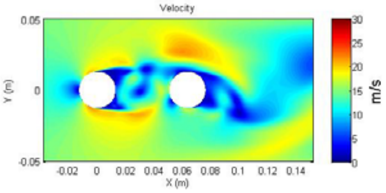

(a) Cross flow model, velocity magnitude.

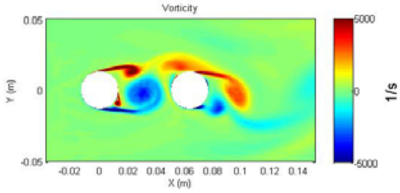

(d) Cross flow model, vorticity magnitude.

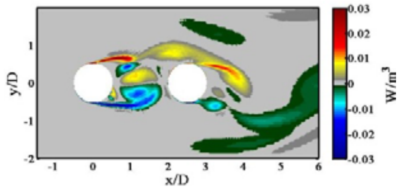

(g) Cross flow model, spatial distribution acoustic power.

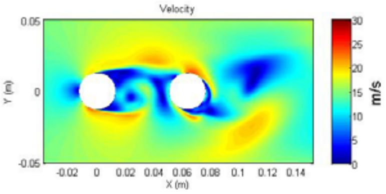

(b) Rigid body vibration model, velocity magnitude.

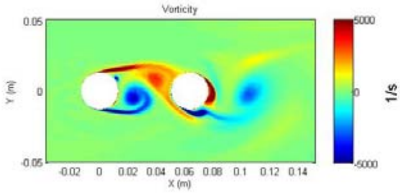

(e) Rigid body vibration model, vorticity magnitude

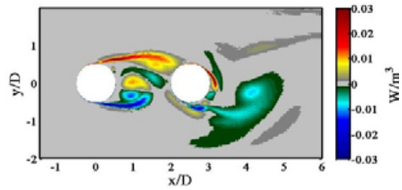

(h) Rigid body vibration model, spatial distribution acoustic power.

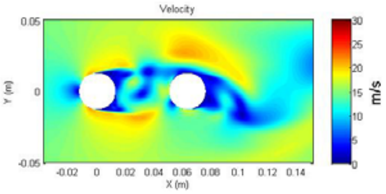

(c) Surface acoustic flow model, velocity magnitude.

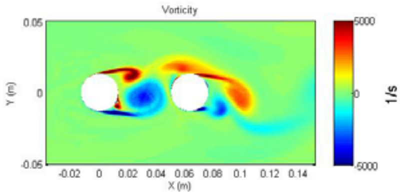

(f) Surface acoustic flow model, vorticity magnitude

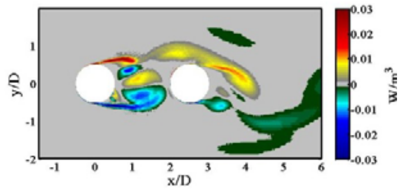

(i) Surface acoustic flow model, spatial distribution acoustic power

Figure 9. Comparison of profile results for the three boundary conditions at coincidence acoustic resonance *fa/fv*=0.95 at phase of 0^o of acoustic particle velocity.

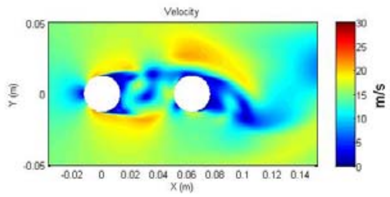

(a) velocity magnitude, phase 0°.

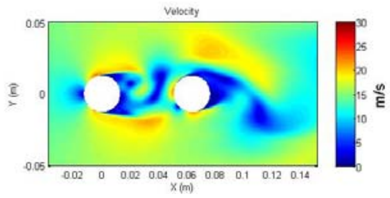

(b) velocity magnitude, phase 45°.

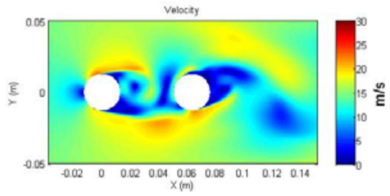

(c) velocity magnitude, phase 90°.

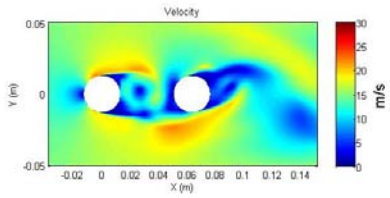

(d) velocity magnitude, phase 135°.

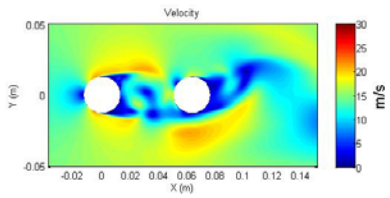

(e) velocity magnitude, phase 180°.

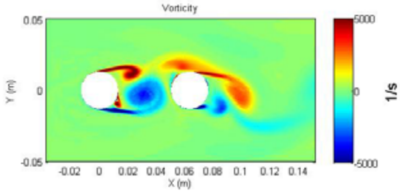

(f) vorticity, phase 0°.

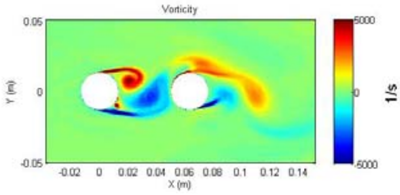

(g) vorticity, phase 45°.

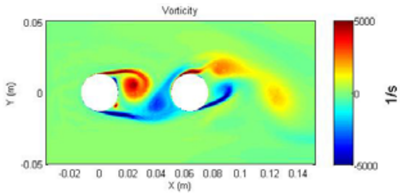

(h) vorticity, phase 90°.

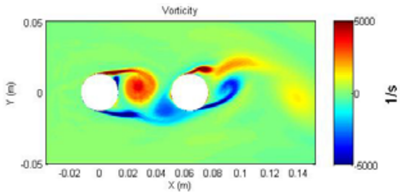

(i) vorticity, phase 135°.

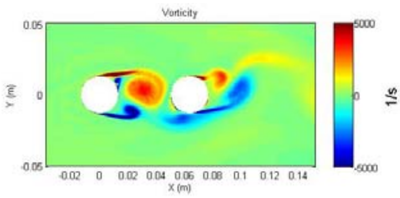

(j) vorticity, phase 180°.

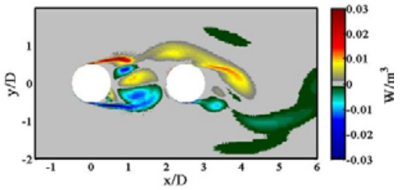

(k) acoustic power, phase 0°.

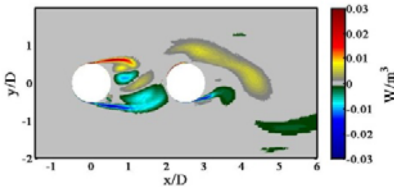

(l) acoustic power, phase 0°.

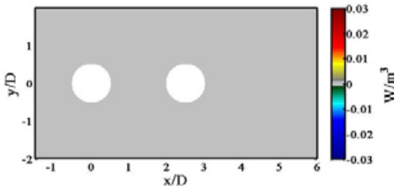

(m) acoustic power, phase 0°.

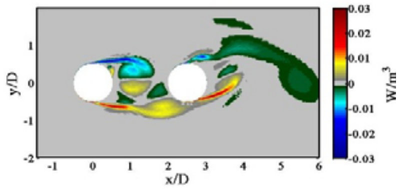

(n) acoustic power, phase 0°.

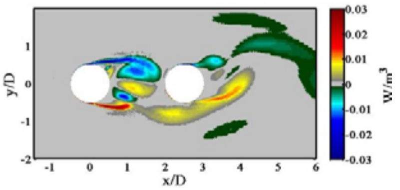

(o) acoustic power, phase 0°.

Figure 10. Phase average profiles for velocity magnitude, vorticity and acoustic power for half-cycle at pre-coincidence acoustic resonance *fa/fv*=1.05 and “surface acoustic flow” boundary condition.

Net acoustic power distribution. Figure 11 shows the net acoustic energy summed over a single period for each of the three boundary conditions considered for a pre-coincidence condition. The particular amplitude for each has been chosen to exhibit comparable acoustic power intensity. As can be seen, all three are qualitatively similar with a large acoustic sink in between the cylinders, and substantial acoustic sources around the nominal shear layers. The rigid body vibration model predicts a very strong source immediately behind the downstream cylinder. The cross-flow model and the surface acoustic flow model are very similar. In general, the cross flow model appears to be generating more intense source regions especially behind the upstream cylinder, but the overall spatial distribution is comparable.

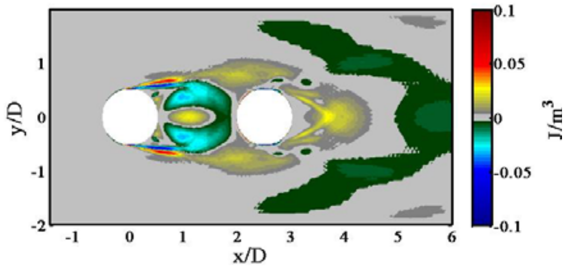

(a) Cross flow model, net acoustic energy summed over a single period;

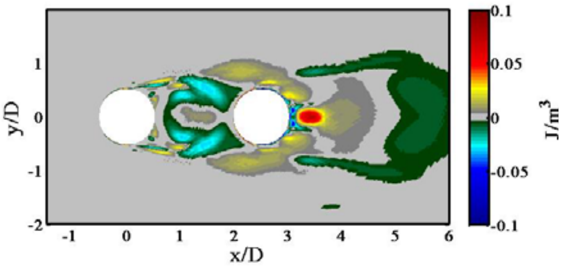

(b) Rigid body vibration model, net acoustic energy summed over a single period.

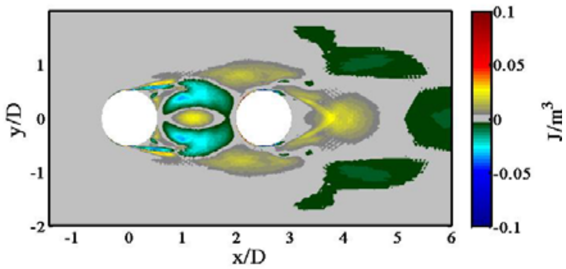

(c) Surface acoustic flow model, net acoustic energy summed over a single period.

Figure 11. Net acoustic energy for pre-coincidence resonance (f_a/f_v=1.05), for each boundary condition.

Figure 12 presents the spanwise summation of the net acoustic energy for the three models. The centre of the upstream cylinder is at *x/D*=0, the centre of the downstream cylinder is at *x/D*=2.5. All three models are comparable in the inter cylinder region, indicating that the higher intensity source regions are less significant than the weaker, but larger source and sink regions. In the wake region, the cross flow and surface acoustic flow models are still broadly in agreement with a strong net sink in the the near wake region. The rigid body vibration model, however, is markedly different. Comparing these distributions with the those obtained experimentally by Finnegan et al.[3] indicate that the cross-flow and the surface acoustic flow models are properly capturing the effect of acoustic excitation, at least qualitatively.

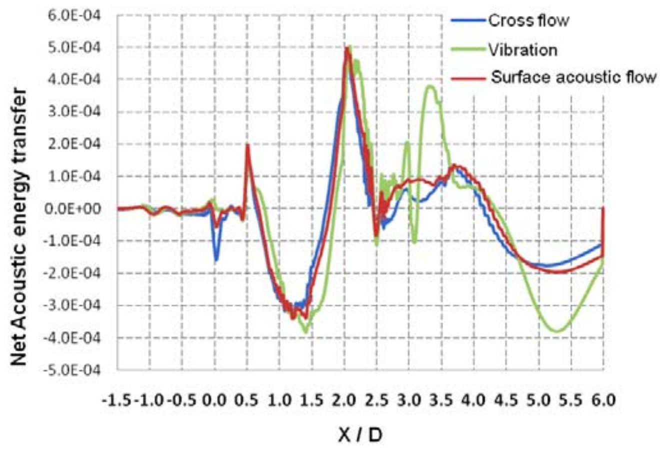

Figure 12. Spanwise summation of net acoustic energy for pre-coincidence resonance, for each boundary condition.

The behaviour of the three models at coincidence is shown in Figure 13. In this, the cross flow and surface acoustic flow models are still in broad agreement. In addition, there are several small sources and sinks immediately behind the downstream cylinder in the cross flow model. The rigid body vibration model yields a dramatically different acoustic power distribution. The difference in the behaviour of the rigid body vibration model is seen more clearly in the spanwise summation of acoustic power shown in Figure 14. The cross flow and surface acoustic flow model again are comparable in the inter cylinder region, although all three models behave differently in the wake behind the two cylinders. At this stage, it is not clear which is correct. Further comparative study with the experimental data of Finnegan et al. [3] is required.

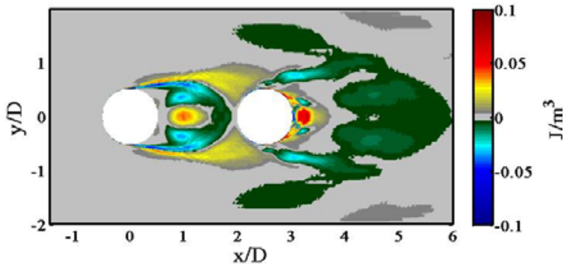

(a) Cross flow model, net acoustic energy summed over a single period;

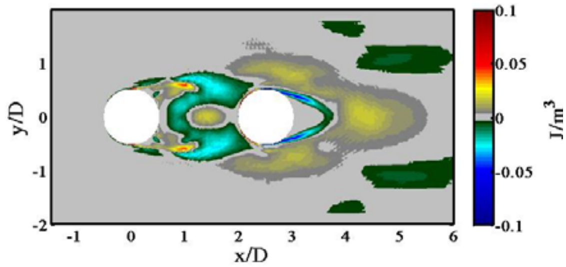

(b) Rigid body vibration model, net acoustic energy summed over a single period.

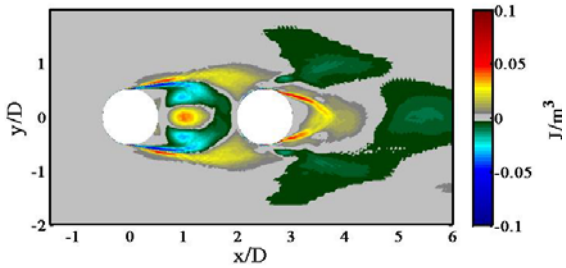

(c) Surface acoustic flow model, net acoustic energy summed over a single period.

Figure 13. Net acoustic energy for coincidence resonance (f_a/f_v=0.95), for each boundary condition.

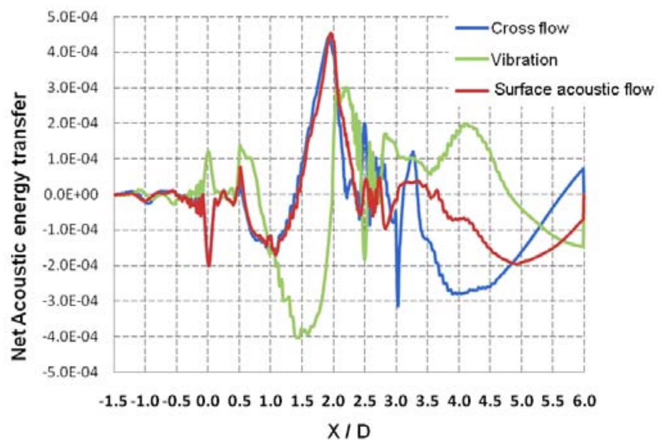

Figure 14. Spanwise summation of net acoustic energy for coincidence resonance, for each boundary condition.

Lock-in region. The three models have been used to investigate the extent of the lock-in region. Figures 15, 16 and 17 show the lock-in map for the three models. Each point represents a single simulation at a given frequency ratio and excitation amplitude. A locked-in regime is marked with a diamond, while a not locked-in regime is marked as a triangle. Both the surface acoustic flow model and the rigid body vibration model exhibit lock-in at a lower excitation amplitude than the cross-flow model, suggesting that exciting the entire flow field effectively adds damping. The surface acoustic flow model appears to have a narrower lock-in region than either of the other two models. However, additional simulations are needed to complete the lock-in map and to determine the lower amplitude bound for resonance and the extent of the lock-in region for the surface acoustic flow model.

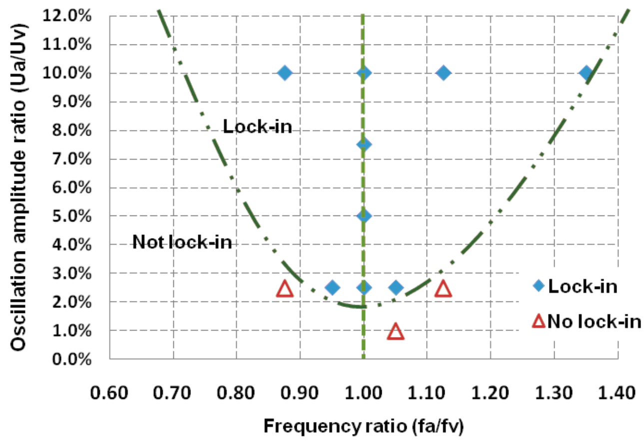

Figure 15 Cross flow model, "lock-in" map.

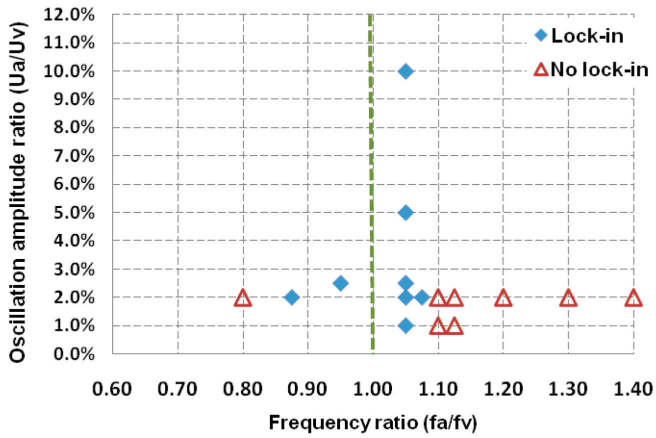

Figure 16. Rigid body vibration model, "lock-in" map.

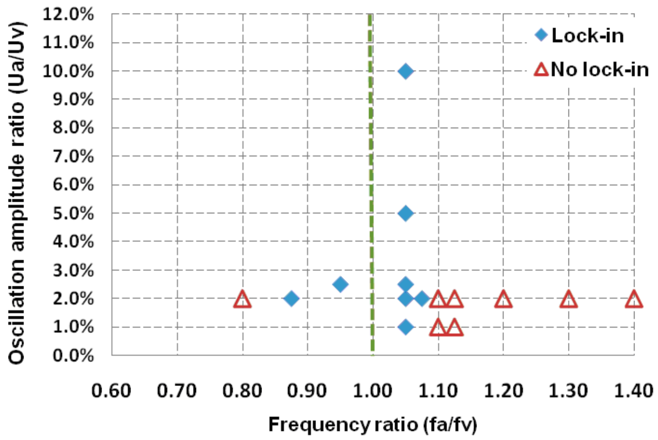

Figure 17. Surface acoustic flow model, "lock-in" map.

CONCLUSIONS

Three different boundary conditions have been implemented to simulate the effect of acoustic resonance on the hydrodynamic field. The rigid body vibration model was found not to be an accurate behavioral representation of acoustic resonance. The cross-flow condition and the flow around the cylinder condition offer qualitatively very similar results. Thus, it is initially concluded that the flow around the cylinder model is a suitable alternative for acoustic resonance simulations. This alternative boundary condition will be easier to implement for complex geometries (e.g. tube arrays). Nonetheless, further validation studies are needed to demonstrate completely the suitability of the new modeling approach.

The initial success of the new boundary condition implies that the coupling between the acoustic field and the hydrodynamics is not reorganizing the wake directly, but rather simply modifying the generation of vorticity at the surface. Furthermore, given that the applied surface velocity in this boundary condition is zero at the top and bottom of the cylinders, it would seem that the main issue in coupling the acoustic field and the hydrodynamics is the windward and leeward region of the tubes. It is conjectured, that the phase between these four location (θ=0,180^o on each cylinder) is critical, although further work is required to investigate this.

REFERENCES

[1] Mohany, A., and Ziada, S., 2009. "Numerical simulation of the flow-sound interaction mechanisms of a single and two-tandem cylinder in cross-flow". *Journal of Pressure Vessel Technology, ASME*, vol. 131, pp.1-11.

[2] Hall, J. W., Ziada, S., and Weaver, D. S., 2003, "Vortex-shedding from single and tandem cylinders in the presence of applied sound". *Journal of Fluids and Structures*, 18, pp. 741-758.

[3] Finnegan, S., Meskell, C., and Ziada, S., 2009. "Experimental investigation of the aeroacoustic sources in a tandem cylinder configuration". *Proceedings of the ASME Pressure Vessels and Piping Division Conference*, ASME, pp. 1-10.

[4] Mohany, A., and Ziada, S., 2009. "A parametric study of the resonance mechanism of two tandem cylinders in cross-flow". *Journal of Pressure Vessel Technology, ASME*, vol. 131, pp. 1-9.

[5] Mohany, A., and Ziada, S., 2005. "Flow-excited acoustic resonance of two tandem cylinders in cross-flow". *Journal of Fluids and Structures*, 21, pp. 103-119.

[6] Fitzpatrick, J. A., 2003. "Flow/acoustic interactions of two cylinders in cross flow". *Journal of Fluids and Structures*, 17, pp. 97-113.

[7] Mohany, A., 2006. "Flow-sound interaction mechanisms of a single and two tandem cylinders in cross-flow". PhD thesis, McMaster University.

[8] Tan, B.T., Thompson, M.C. and Hourigan, K., 2003. "Sources of acoustics resonance generated by the flow around a long rectangular plate in a duct". *Journal of Fluids and Structures*, 18, pp. 729-740.

[9] Hourigan, K., Welch, M.C., Thompson, M.C. and Stokes, A.N. (1990) "Aerodynmic sources of acoustic resonance in a duct with baffles". *Journal of Fluids and Structures*, 4, pp. 345-370.

[10] Howe, M. S. (1980) "The dissipation of sound at an edge," *Journal of Sound and Vibration*, Vol. 70, No. 3, pp. 407–411, DOI: 10.1016/0022-460X(80)90308-9.